UNC-5075

THE USE OF GAMMA PROBING TO DETERMINE THE SHIELDING EFFECTIVENESS OF SPACE VEHICLES

A. D. Krumbein
F. Johnson

Project Scientist: A. D. Krumbein

February 18, 1964

Work Performed under UNC Project 2193
Contract No. NAS 8-5252 with
George C. Marshall Space Flight Center,
NASA, Huntsville, Alabama

UNITED NUCLEAR
CORPORATION

DEVELOPMENT DIVISION

UNC-5075

THE USE OF GAMMA PROBING TO DETERMINE THE SHIELDING EFFECTIVENESS OF SPACE VEHICLES

A. D. Krumbein
F. Johnson

Project Scientist: A. D. Krumbein

February 18, 1964

Work Performed under UNC Project 2193
Contract No. NAS 8-5252 with
George C. Marshall Space Flight Center,
NASA, Huntsville, Alabama

UNITED NUCLEAR CORPORATION
Development Division
White Plains, New York

ABSTRACT

The feasibility and practicality of using a gamma-ray probe technique to determine the shielding effectiveness of various material configurations against proton radiation has been demonstrated. The experimental technique and calculational procedure involved are explained, and results are given for simple arrays and actual pieces of space equipment.

CONTENTS

1. SUMMARY 1

2. INTRODUCTION 3

3. THE GAMMA-PROBE TECHNIQUE 9
   3.1 Principles of the Method. 9
   3.2 The Experimental Method 11
      3.2.1 Energy Discrimination 12
      3.2.2 The Effective Compton Cross Section 13

4. CALCULATION OF PROTON DOSE. 17
   4.1 The Calculational Procedure. 17
   4.2 Comparison With Analytical Results 19

5. EXPERIMENTAL RESULTS USING UNCOLLIMATED GEOMETRY . . 23

6. PROTON DOSE AND THE ATOMIC NUMBER OF THE ATTENUATING MATERIAL 29
   6.1 General Considerations 29
   6.2 Selection of an "Average" Proton Attenuating Material for the Dose Calculations 30

7. THE EFFECT ON DOSE CALCULATIONS OF THE VARIATION OF SEVERAL SYSTEM PARAMETERS 33
   7.1 Gamma-Ray Source. 33
   7.2 Scintillator Crystal Size. 34
   7.3 Mesh Size 36
   7.4 Source-Sample-Detector Distances 38

8. GAMMA-PROBE TECHNIQUE AND HOMOGENIZATION. 43

9. CONCLUSIONS 47

10. APPENDIX – DESCRIPTION OF THE AUTOMATIC SCANNING SYSTEM. 49
   10.1 The Scanning Table 49
   10.2 The Counting and Recording System 52

11. REFERENCES 55

TABLES

1. The Effective Compton Cross Section as Measured for a Number of Materials for Co^{60} Gamma Rays 15
2. The Effective Compton Cross Section as Measured for a Number of Aluminum Thicknesses for Co^{60} Gamma Rays 15
3. Sample Spectra Used in PROBE Code 20
4. Comparison of Dose Calculated Analytically with PROBE Code Calculations, for the May 10, 1959 Solar Flare. 21
5. Dose from NASA Equipment – SA 105 24
6. Comparison of Doses Obtained in Moving Source Geometry With Those from Moving Sample Geometry. 26
7. Proton Dose Results Using Several Range-Energy Tables – NASA Voltage Supply Box Scanned in Collimated Geometry 31
8. Proton Dose Results, Using Several Range-Energy Tables – As Calculated for Several Thicknesses of Aluminum 32
9. Theoretical and Effective Compton Cross Sections for Co^{60} and Cs^{137} . 34
10. Doses Behind an Array of 1-in. Al Blocks Spaced 1 in. Apart – Variation With Crystal Size 35
11. Doses Behind an Array of 1-in. Al Blocks Separated by 1/8, 1/4, 1/2, and 1 in. Spaces – Variation With Crystal Size. 35
12. Doses Behind NASA SA 105 Equipment – Variation With Mesh Size . 37
13. Dose Behind North American Aviation Space Vehicle Sections – Variation With Mesh Size 37
14. Dose Behind an Array of 1-in. Al Blocks Separated by 1/8, 1/4, 1/2, and 1 in. Spaces (1 in. $\times$ 1 in. Crystal) – Variation With Source-Sample-Detector Distance 42
15. Comparison of Calculated Dose Based on Homogenized Density With Calculated Dose Based on Gamma-Probe Scans 44

FIGURES

1. Stopping Power for Protons, $S = -(1/\rho)(dE/dx)$ 5
2. Stopping Power for Protons in Terms of Electron Density. 6
3. Results of a Gamma-Ray Scan of a 1-in. Al Cube Array Spaced 1/8, 1/4, 1/2, and 1 in. 39
4. Results of a Gamma-Ray Scan of a 1-in. Al Cube Array Spaced 1/8, 1/4, 1/2, and 1 in. with the Addition of 1/4 in. of Al in Front of the Source and in Front of the Detector 40
5. The Gamma-Probe Scanning System 50
6. Schematic of the Scanning Table Drive Mechanisms 51
7. Block Diamgram of the Electronics System 53

1. SUMMARY

The major objective of the program described in this report is to determine the feasibility and practicality of using a gamma-ray probe technique to determine the shielding effectiveness of various material configurations against proton radiation. The essence of the technique is the use of gamma-ray attenuation measurements to determine the areal electron densities at a number of cross sections through the material configurations. A calculational procedure, in the form of a machine code, is then used to calculate the proton dose received behind these configurations from typical proton spectra found in space. The energy loss per electron is used rather than energy loss per gram.

As a result of the study described in this report, it is concluded that the gamma-ray probe method of obtaining proton dose is both feasible and practical. It is felt that it can be used to determine the proton dose inside actual space vehicles with good accuracy and in a reasonable amount of time. Experiments performed with pure materials, simple arrays, and actual space capsule components demonstrate this feasibility.

In order to make the method practical for a large vehicle, i.e., to reduce the time required, uncollimated geometry must be used relying only upon energy discrimination to determine the unscattered portion of the gamma-ray beam. Comparisons between collimated and uncollimated scans of actual space vehicle components give, at most, a difference of 30% in the estimates of the proton dose. This uncer-

certainty is for a proton flare spectrum having a large number of low-energy protons where a strong dependence of dose on fairly small variations in material thickness would be expected. For other flares, and for Van Allen belt protons, the difference between the collimated and uncollimated dose results has never been found to be greater than 10%.

It has been possible to resolve narrow openings or thin spots in the simple arrays and pieces of apparatus studied, as long as the mesh size used in the particular probing scan is of the same order of magnitude as the width of the opening. Dose values, however, proved to be fairly insensitive to mesh size for the space capsule components studied. Experiments with mesh sizes from 0.1 in. $\times$ 0.1 in. to 1 in. $\times$ 0.5 in. give less than 10% difference in calculated proton dose.

Since the exact materials which comprise the particular sections to be probed may not be known because of the inhomogeneity of the components, the proper proton stopping power might not be used in the dose calculations. It is shown, however, that the use of an "average" proton stopping power or range-energy table gives a reasonably correct proton dose as long as the components probed do not contain large amounts of material with atomic numbers greater than 30, i.e., above copper in the periodic table.

2. INTRODUCTION

The presence of penetrating radiations in space necessitates the protection of the crew of space vehicles by some sort of radiation shielding. In all cases envisioned at present, the space vehicle structure and equipment will provide the only real protection against a lethal radiation dose if astronauts are caught in midpassage by a solar proton flare. Therefore, the vehicle designers and NASA must have an accurate evaluation of the actual radiation protection offered by a spacecraft prior to its use.

This information will be valuable in showing up inadequacies in the shield which may be corrected by rearrangement of equipment or "spot shielding" of unusually thin portions. Even if such rectification is not feasible, the astronauts will at least know the extent of the possible radiation dose they may encounter during the course of their journey. Such knowledge also may influence any decision to return the flight short of its destination if the appearance of a large solar flare is believed to be imminent.

Present analytic evaluations of the shielding effectiveness of vehicle structure and components can only handle space vehicle areas in homogeneous form. This necessitates the homogenization of the spacecraft equipment. Even if the machine codes which perform the shielding calculations could treat a large number of small spacecraft areas, the structural information needed to give the proper dose results, particularly for the equipment, is just not available for use in such codes.

The equipment and structure in these areas would still have to be homogenized, leading in many cases to the calculation of doses to the astronauts lower than those which might actually be encountered in a space environment.

However, preliminary studies at United Nuclear have shown that inhomogeneities could result in dose factors of two or more higher than expected for the same total average areal density of material. Therefore, it was felt that a more precise evaluation of the shielding effectiveness of the space vehicle structure and equipment was needed to insure adequate radiation protection for the astronauts.

An intensive study of the radiation environment to be encountered in space has indicated that the predominant radiation hazard is from high-energy protons.[1,2] Moreover, the main energy loss mechanism of protons in the energy range encountered in space is by ionization of the attenuating material,[3] and is, therefore, a function of the number of electrons in the path of the proton beam. Since this is so, a method which can measure the areal electron density encountered by the incident protons will furnish the proper information for use in calculating proton attenuation. In fact, as Figs. 1 and 2 show, if several materials are involved, proton attenuation is better characterized by the number of electrons in the path of the protons than by the total mass of material.

As a result of work over the past several years, United Nuclear has developed a gamma-ray technique for measuring areal electron density along paths through material structures and equipment. This method is based on measurements of the attenuation of gamma rays through the samples of interest. The gamma-ray energy is selected so that the chief attenuation process is Compton scattering. Since, in the Compton process, the electrons act as though they are unbound, the cross section per atom is equal to the cross section per electron (a constant) times the number of electrons per atom. In this way, then, the attenuation of gamma rays undergoing Compton scattering can be used as a measure of the areal electron density of the attenuating medium.

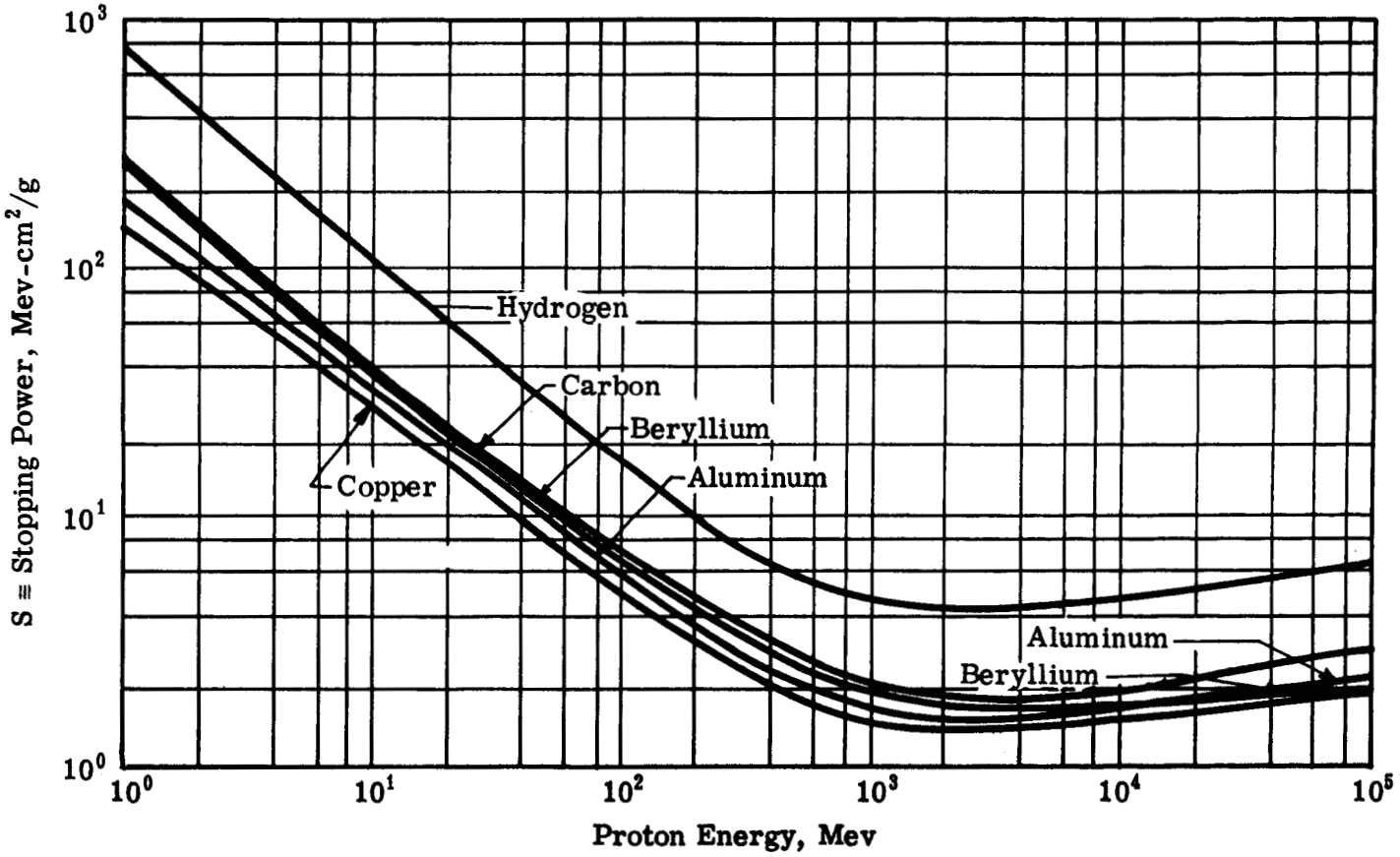

Fig. 1 — Stopping power for protons, $S = -(1/\rho)(dE/dx)$

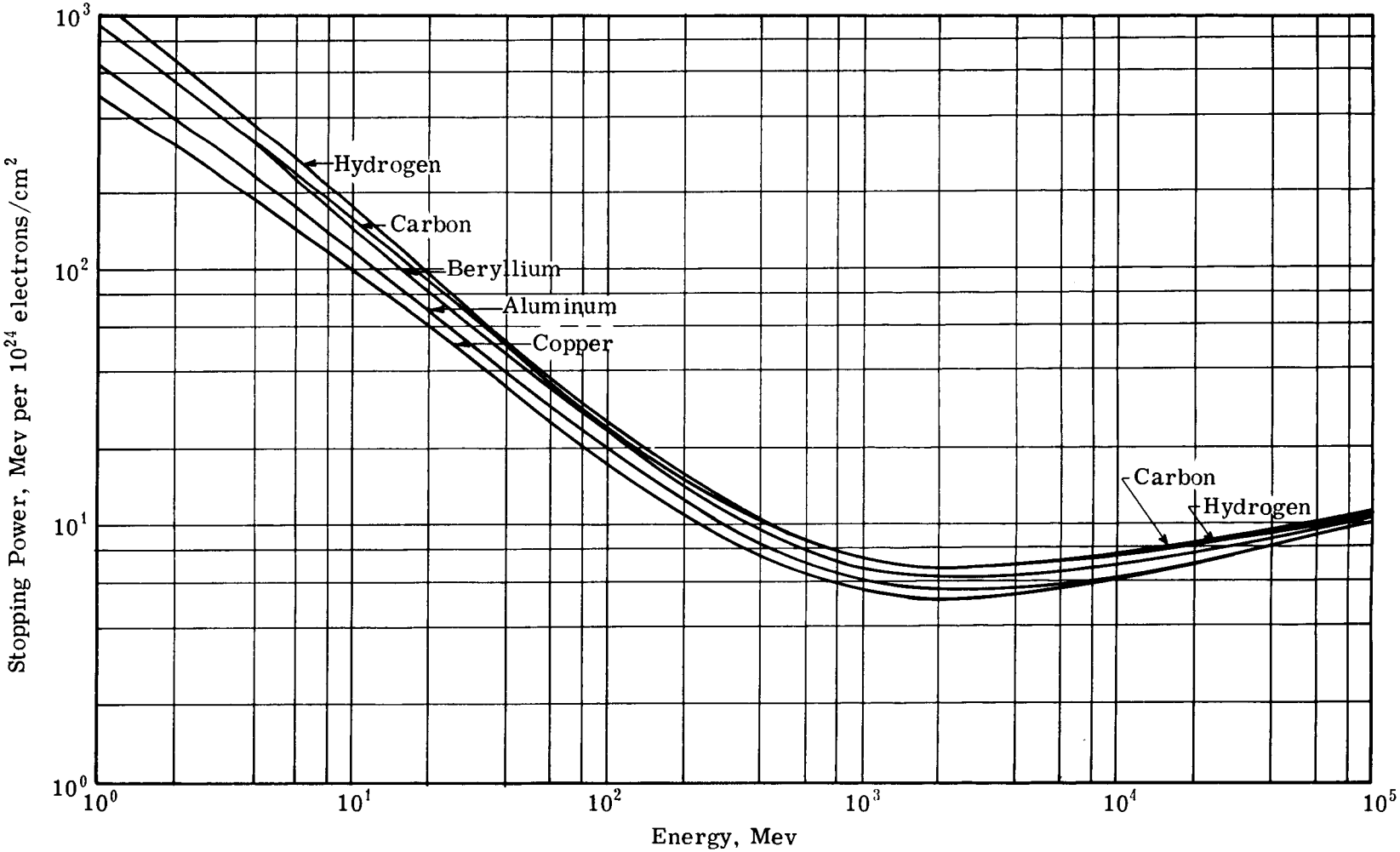

Fig. 2 — Stopping power for protons in terms of electron density

Having obtained the areal electron density along a large number of paths through the structure and/or equipment of interest, one can calculate the proton dose from typical proton spectra likely to be encountered in space. Depending on the dose model used, average body or surface dose can be calculated (although in this study calculations are restricted to the former).

For the real, inhomogeneous capsules and vehicles to be studied, tens to hundreds of thousands of paths would have to be scanned. Therefore, it would be impractical in terms of time and equipment to use collimation for the measurement of the unscattered portion of the transmitted gamma-ray beam. Rather, the use of uncollimated geometry was investigated, relying upon energy discrimination alone in the measurements. One of the major tasks in the present study was aimed at evaluating the accuracy of the uncollimated gamma-probe technique.

Another problem requiring solution before the technique could be used to probe inhomogeneous samples was the practicality of using a single stopping power or range-energy table to calculate proton attenuation. As Fig. 2 shows, even if electron density is used, there is still some variation of proton attenuation with the atomic number of the material. The analysis of this problem also was undertaken in the study.

Section 3 of this report explains the principles of gamma probing in detail and describes briefly the experimental method used. Section 4 describes the calculational method evolved to determine proton dose from the measured electron densities. Section 5 describes the experiments performed and analysis made using uncollimated geometry, and how the results compared with several collimated cases. Section 6 describes the results of using different range-energy tables for proton attenuation. Section 7 gives the results of varying such parameters as the gamma-ray source, crystal size, mesh size, and source-sample-detector distances. The effects of the last named on the resolution of structure are given also. Section 8 describes calculations which show the apparent degree of homoge-

neity, based on the gamma-probe results, of actual pieces of spacecraft equipment and structure.

It is concluded, in Section 9, that based on the results of this program, the feasibility and practicality of using the gamma-probe method for the determination of the shielding effectiveness of space vehicles and their equipment is demonstrated.

3. THE GAMMA-PROBE TECHNIQUE

3.1 PRINCIPLES OF THE METHOD

The principal phenomenon by which the energy of a proton is attenuated in a shield is by ionization of the stopping material. This holds true up to proton energies of at least 300 Mev, and since the largest proportion of the dose received from protons in space is contributed by protons below this energy,[3] the ionization loss is the only one considered in the present study.

The shielding ability of a material is measured by its stopping power, S, defined as

$$S(E) = \frac{1}{\rho}\frac{dE}{dx} \quad \text{Mev/g/cm}^2 \tag{1}$$

where ρ is the density of the material in g/cm^3. The stopping powers of a number of materials, which are typical of those to be used in space vehicle equipment, are given in Fig. 1.

As indicated in Fig. 1, the stopping powers of different materials show considerable variation. Fig. 2 shows data for the same substances with the stopping powers put in terms of $Mev/10^{24}$ electrons/cm^2 (in this case ρ is the electron density in 10^{24} electrons/cm^3 rather than the mass density). It is clear that, if several materials are involved, proton attenuation is better characterized by the number of electrons placed in the path of a proton beam than by the total mass of the shield material.

The basic problem in evaluating the proton dose at a point inside a vehicle is the determination of the number of electrons along each ray which arrives at that point from outside the vehicle. With this information, the energy loss of a proton following any path to the dose point can be calculated. Thus, the spectrum of protons hitting the dose point (and from this the dose itself) is calculable if the spectrum incident on the vehicle is known. The theory of the gamma-probe technique for determining the number of electrons along each ray is presented below.

In passing through matter, a gamma photon can undergo three important interactions: photoelectric absorption, pair production, and Compton scattering. For elements with Z less than 50, the Compton scattering process represents more than 94% of the total cross section at the energies of the Co^{60} gammas (1.17 and 1.33 Mev). For gamma rays from Cs^{137} (0.67 Mev) Compton scattering accounts for more than 88% of the cross section for Z up to 50. Most of the materials likely to be used in space vehicles have Z below 30 and in this range the Compton process represents more than 98% of the cross section, even for Cs^{137} gammas.

In the Compton scattering process, the photon scatters off one of the atomic electrons, changes its direction, and loses an amount of energy related to the deflection angle by the well-known Klein-Nishima formula. In this process the electrons act as though they were unbound, and the cross section per atom is equal to the Compton cross section per electron times the number of electrons per atom. The attenuation of gamma rays in the energy range of those from Co^{60} and Cs^{137} is, therefore, a measure of the areal electron density, i.e., electrons/cm^2 of the attenuating medium.

If I_0 gamma-ray photons per unit area are incident on a thickness, t, of material, then the number, I, of these photons which penetrate that thickness without having undergone a Compton scattering is given by

$$I = I_0 \exp\left(-\int_0^t N_e \mu_e \, dt\right) \tag{2}$$

where N_e is the number of electrons per unit volume of material and μ_e is the Compton cross section per electron. Since μ_e is independent of material, it can be removed from the integral, thus reducing the integral to the number of electrons per unit area normal to the gamma-ray beam. Then a transmission measurement in which one measures the number of transmitted photons which have not suffered Compton scattering gives the areal electron density from the relationship

$$\int_0^t N_e \, dt = \frac{1}{\mu_e} \ln \frac{I_0}{I} \tag{3}$$

Since Compton scattering changes the direction of motion and at the same time reduces the energy of the photon, the unscattered portion of the transmitted beam can be determined either by collimation or by energy discrimination, or by a combination of both techniques.

The values for μ_e appearing in Eq. 3 can be found in Reference 4. For Cs^{137}, a value of 0.254×10^{-24} cm^2/electron is listed, while for Co^{60} an average value for the two gamma rays of 0.186×10^{-24} cm^2/electron was obtained. These values were checked experimentally on a 3/4-in. piece of aluminum using, simultaneously, good collimation and energy discrimination. The number of electrons/cm^2 calculated using Eq. 3 and transmission measurements were within fractions of a percent of those actually present.

3.2 THE EXPERIMENTAL METHOD

In its simplest form, the experimental configuration consists of a gamma source (Co^{60} or Cs^{137}), an NaI (Tl) crystal detector, and a single-channel pulse height analyzer and scaler. A positioning or traversing device to locate accurately or to move the sample between source and detector also is required. Additional voltage

stabilization requirements, necessitated by our reliance on energy discrimination only, will be discussed in the next section.

The experiments conducted as part of this program were performed both manually and automatically. In the former, the sample was moved in set increments between the fixed source and detector, while in the automatic operation either the sample or the source was moved. In all cases, two fundamental measurements were taken, viz., I_0, the gamma-ray intensity at the detector with no sample interposed, and the transmitted intensity, I, when the sample is between the source and the detector. Having the values of I and I_0, the areal electron density can be calculated using Eq. 3.

Other parameters varied in the experiments, besides the gamma-ray source, were: (1) crystal size, (2) source-sample-detector distances, and (3) mesh or grid size. The last was accomplished in the automatic equipment by having the scanning table move horizontally until a preset distance was traversed, move vertically a small preset distance, and then traverse horizontally in the opposite direction. This procedure is repeated until the entire surface of the sample is scanned.

The details of the construction of the scanning table and of the associated electronic equipment are given in the Appendix (Section 10).

3.2.1 Energy Discrimination

Since one aim of this study was to ascertain the feasibility of using the gamma-probe technique in uncollimated geometry, the experimental method made use of energy discrimination almost exclusively. Ideally, in this method the pulse height analyzer would be set to record only those gamma pulses in the full energy peak of the pulse height spectrum, thereby detecting, to a high degree of accuracy, only the unscattered gamma rays. However, since in practice the energy peak has finite width, a finite "window" size must be used. At the same time, the discriminator of the system must be set at the lower end of the peak, at a value where

changes in discriminator level caused by noise or drift will have the least effect on the observed counting rate. Since measurements are made over a fairly long period of time (several hours), drift errors become very important. For that reason, a voltage stabilizing device known as a "Spectrastat" was used to hold the discriminator setting at a predetermined value.

In the early stages of the program it was found that considerable loss of counts occurred at the counting rate employed (several thousand counts per second), when pulse height analysis was used. It was ascertained that the dead time of the analyzer was not insignificant, and therefore, integral discrimination was substituted for pulse height analysis. Using this method, no dead time losses were incurred up to at least 10,000 counts per second and good counting statistics were obtained. At the same time, no significant number of higher energy pulses were counted when the window was made infinitely wide. Integral discrimination then was used throughout the remainder of the experimental program.

Incidentally, when Co^{60} was used as a source, the discriminator was set at the minimum of the lower peak, thus including counts from both peaks. This was done mainly to increase the counting rate as no other difference could be discerned between this situation and setting the discriminator at the minimum of the higher peak (E = 1.33 Mev).

3.2.2 The Effective Compton Cross Section

The need to set the discriminator at a certain energy below the peak leads to the acceptance of scattered gamma rays by the counting system. If there is no collimation to block the entrance of these scattered rays to the detector, they will result in spuriously high transmitted counting rates making it appear as if the shielding material were thinner than it is.

In order to calculate the angle through which a gamma ray can scatter and still be counted, the following formula is used, which follows from the theory of the

Compton effect:

$$E' = \frac{E}{1 + E(1 - \cos \theta)} \tag{4}$$

where E is the energy of the gamma ray in units of electron rest mass (0.511 Mev) and E′ is the energy of the same gamma after scattering through an angle θ.

For the Co^{60} source, where E_{γ_1} = 1.17 Mev and E_{γ_2} = 1.33 Mev, the discriminator was set at 1.07 Mev which is the value of E′ to be used in Eq. 4. Eq. 4 shows that these gamma rays, when scattered through angles of 17° and 25°, respectively, still will be accepted by the counting system. For Cs^{137}, where E_γ = 0.67 Mev, E′ is set at 0.58 Mev and rays scattered through as much as 27° are accepted by the system.

One can compensate for this "inscattering effect" by determining experimentally an effective Compton cross section, μ_{eff}, which will lead to the correct shield thickness or areal electron density when used with the observed gamma-ray transmission in Eq. 3.

An effective value of μ for various materials for a single thickness has been obtained as well as for various thicknesses of aluminum. Table 1 gives the measured values of effective Compton cross section for several materials from paraffin to uranium. It will be noted that up to at least Z = 30 a single μ_{eff} appears to fit all the materials. The value used is 0.150×10^{-24} cm^2/electron. Similar experiments with Cs^{137} led to a value of μ_{eff} of 0.174×10^{-24} cm^2/electron. Table 2 gives the results of the experiments with various thicknesses of aluminum for a Co^{60} source. Here too, a single value of μ_{eff} emerges, averaging about 0.154×10^{-24} cm^2/electron over the entire range, but giving the smaller value of 0.150×10^{-24} in the vicinity of the 5.6 g/cm^2 used to obtain the values in Table 1. Since most of the scanned samples have had an average density less than 7 g/cm^2, the lower value of μ_{eff} (0.150) is used in the calculations.

Table 1 — The Effective Compton Cross Section as Measured for a Number of Materials for Co^{60} Gamma Rays

Material*	Atomic No.	μ_{eff} cm^2/electron
Paraffin		0.147×10^{-24}
Al	13	0.150×10^{-24}
Ni	28	0.148×10^{-24}
Cu	29	0.152×10^{-24}
W	74	0.187×10^{-24}
Pb	82	0.193×10^{-24}
U	92	0.222×10^{-24}

*The thicknesses used are those equivalent to 2 cm of Al (5.58 g/cm^2).

Table 2 — The Effective Compton Cross Section as Measured for a Number of Aluminum Thicknesses for Co^{60} Gamma Rays

Aluminum		μ_{eff},
in.	g/cm^2	cm^2/electron
0.25	1.77	0.152×10^{-24}
0.50	3.54	0.150×10^{-24}
1.0	7.09	0.154×10^{-24}
1.5	10.6	0.151×10^{-24}
2.0	14.2	0.155×10^{-24}
3.0	21.3	0.157×10^{-24}
4.0	28.4	0.156×10^{-24}

4. CALCULATION OF PROTON DOSE

4.1 THE CALCULATIONAL PROCEDURE

The gamma-ray probing measurements, as discussed in Section 3, produce two pieces of experimental data for each path traversed, viz., I_0, the gamma-ray intensity in the absence of the sample under test and I, the intensity transmitted through the sample. These two pieces of information, when combined with a suitable value of the Compton cross section per electron, enable us to calculate the electron density along the particular path by use of Eq. 3.

Once the electron density is calculated, the gamma-ray measurements have served their purpose and all further calculation are concerned with proton attenuation. A calculational procedure is now used which transforms electron densities into average proton body dose. The remainder of this section is devoted to a brief description of that procedure. A FORTRAN machine code, PROBE, was written to perform the dose calculations. The main code solves the dose problem for the case of a fixed source and detector and a moving sample. In addition, a modification of the original code enables the calculation of the dose for moving source, fixed sample-detector configurations.

The calculation is begun by choosing an incident proton of energy E_{min}, from a given spectrum and determining its range, R(E), from a range-energy expression or table. (The range-energy tables to be used in particular cases and the reasons for their use will be discussed in Section 7.) The range of the proton after

traversing each measured path, i, is calculated by means of the simple expression

$$R_i(E') = R(E) - N_i \tag{5}$$

where N_i is the electron density, in electrons/cm^2, along the path, i. The proton range, of course, must be given in similar units. The energy, E', of the "degraded" proton is then obtained from its range in the same manner as the reverse process detailed above.

This computation is carried out for all measured paths, i, and for all protons in the given energy spectrum. Of course, since this is a discrete calculation, protons are chosen according to a previously determined energy mesh. This mesh takes into account the relative contributions of particular proton energies to the proton dose.

For each proton of initial energy, E, there is a number of degraded protons of energy E_i'. A dose model is now chosen and the energy losses, ΔE_i, of all the degraded protons originating from a single incident proton of energy, E, in this model are calculated. The method is exactly the same as that used in calculating the degraded proton energy, except that the thickness (or diameter) of the dose model is substituted for N_i in Eq. 5. The energy losses are then averaged over all the "n" paths measured to give an average energy loss over the entire sample for an incident proton of energy, E, viz.,

$$\mathcal{D}(E) = \frac{1}{n} \sum_{i=1}^{n} \Delta E_i \tag{6}$$

Since the important aspect of this study is to compare several methods of measurement and calculation, it was felt that the use of a single dose model would be best. The model chosen, in the moving sample case, is a slab of water 10-cm thick and of the same area as the sample. For the moving source configuration, the model is a water sphere 5 cm in radius, and the protons are all

constrained to pass through the diameter of the sphere. The units of dose can be either Mev or Mev/g. The former is used, however, as it makes comparisons between samples of various sizes more meaningful.

The final step in the calculation is the integration of the average energy losses, $\mathscr{D}(E)$, over the complete proton spectrum, to give the final dose. The proton spectra used were put in the form

$$\phi(E) = K E^{-n} \tag{7}$$

where K and n are constants which are specified for given energy ranges. Table 3 lists the values of K and n employed for the spectra of the three representative solar flares used in this study. In addition, similar values are given for the Van Allen belt proton spectrum as deduced from the paper of Freden and White.[5] The constants for the three solar flares were computed from graphs of the time integrated flare spectra previously obtained at United Nuclear.[6]

For the moving source calculation, a modification needs to be made in Eq. 6 so that the solid angle subtended by the source at the detector is taken into account. Eq. 6 becomes, in this case,

$$\mathscr{D}(E) = \frac{1}{n} \sum_{i=1}^{n} \Delta E_i \cos \theta_i \tag{8}$$

where θ_i is the angle between each measured path, i, and the normal from the fixed detector position to the sample. Otherwise, the calculation proceeds as discussed previously.

4.2 COMPARISON WITH ANALYTICAL RESULTS

Several simple problems were solved analytically and the results were compared with those obtained from the PROBE code. The cases chosen in the moving sample case were: (1) no shield and (2) a uniform 1-in. slab of aluminum. The

Table 3 — Sample Spectra Used in PROBE Code

Energy Range, Mev	K	n
May 10, 1959 Flare		
10-60	1.90×10^{11}	1.5
60-780	3.19×10^{17}	5.0
Sept. 3, 1960 Flare		
10-60	4.03×10^{6}	0.7
60-200	8.00×10^{7}	1.43
200-780	7.87×10^{12}	3.6
Feb. 23, 1956 – Giant Flare		
10-150	8.50×10^{9}	1.5
150-400	5.00×10^{12}	2.65
400-780	2.00×10^{10}	1.73
Van Allen Belt – Freden and White Spectrum		
10-80	1.55×10^{2}	0.72
80-400	7.33×10^{3}	1.60
400-700	1.02×10^{5}	2.04

results for the solar flare of May 10, 1959 are given in Table 4. It is seen that the results are in reasonable agreement.

Although the much more difficult exact analytical calculation was not attempted for the moving source case, the good agreement between all moving sample and moving source computations gives reasonable confidence in the method for the latter case.

Table 4 — Comparison of Dose Calculated Analytically with PROBE Code Calculations, for the May 10, 1959 Solar Flare

	Moving Sample Case (Dose in Mev)	
Shield Thickness	Analytical Result	Code Result
0	2.196×10^{12}	2.198×10^{12}
1 in. of Al	8.852×10^{10}	8.222×10^{10}

5. EXPERIMENTAL RESULTS USING UNCOLLIMATED GEOMETRY

As pointed out in Section 3, when the gamma-ray probe method is used in uncollimated geometry, an effective Compton cross section must be used when calculating electron density. In order to compare these results with those obtained when the system is collimated, a piece of electronic equipment (supplied by MSFC, Huntsville) was scanned in both geometries.

The electronic circuit tested was labeled NASA Equipment Box, SA 105 and was approximately 50 $in.^2$ in area. Collimation was accomplished by placing a lead collimator either 1/4 in. or 1/2 in. in diameter and 4 in. long, in front of the source and a similar collimator 1/2 in. in diameter in front of the detector. As the source itself was only 1/16 in. diameter, it essentially determined the extent of collimation at that end of the system.

Collimators of 1/2 in. diameter and 4 in. long at both source and detector allow an acceptance angle of only 2° for the source-detector distances used (20 in.). Experiments with known thicknesses of aluminum and collimators of these dimensions gave a value for the Compton cross section of 0.186×10^{-24} cm^2/electron, i.e., the theoretical value. Therefore, it is felt that the collimators used do give "good" collimation.

The results of dose calculations made from scan data on this piece of equipment are given in Table 5 for the four proton spectra studied. The theoretical Compton cross section for Co^{60} of 0.186×10^{-24} cm^2/electron is used in calculating the col-

limated values, while an effective value of 0.150×10^{-24} cm^2/electron is used for the computation of the uncollimated results. As can be seen, a maximum difference of about 30% is found between the results of the two types of measurements.

Table 5 — Dose from NASA Equipment, SA 105
Comparison of Collimated and Uncollimated Scans

(Mesh Width: 0.2 in. × 0.2 in.)

	Doses*	
Flare	Collimated Geometry	Uncollimated Geometry
May 10, 1959	3.95×10^{11}	5.25×10^{11}
Sept. 2, 1960	9.92×10^{8}	1.07×10^{9}
Feb. 23, 1956	9.29×10^{10}	9.92×10^{10}
Van Allen belt	4.43×10^{3}	4.70×10^{3}

*The dose units for the solar flares are in Mev; for the Van Allen belt the units are Mev/sec.

This largest difference occurs for the solar flare of May 10, 1959, in which a large number of low energy protons were found. For this proton spectrum, relatively small differences in the values of the calculated electron densities will result in comparatively large differences in dose. A slightly larger calculated electron density than actually exists will appear to stop many low energy protons and prevent them from contributing to the dose. On the other hand, if a slightly smaller electron density is calculated, low energy protons which are actually stopped in the sample will get through, and since they will deposit all their energy in the dose model, will contribute very significantly to the dose. For the other sample spectra used, low energy protons are not as important and the maximum differences obtained between collimated and uncollimated cases do not exceed 10%.

A different type of uncollimated scan also was made, namely, one using a moving source and a fixed detector. This is the system which is best suited for the scanning of a full-scale capsule such as the Apollo command module. With the source moving along the outside of the capsule, a number of detectors can be placed at fixed points inside the capsule and the dose data obtained at all these points simultaneously.

The results of the dose calculations made in moving source geometry as compared with those obtained by the moving sample technique are given in Table 6 for the NASA SA 105 equipment piece, as well as for portions of the Apollo capsule wall. The latter samples, supplied by North American Aviation, are: (1) a stainless steel honeycomb sample, about 3/4 in. thick, bonded to aluminum walls by epoxy resin, (2) a 2-in. thick sample with a stainless steel honeycomb welded to stainless steel walls.

The moving source scans were made with a mesh width (see Section 7.3), of 0.3 in. by 0.3 in. and are, therefore, compared to runs with similar mesh widths using the moving sample method. Hence, there are different values given for the NASA equipment in this table.

As can be seen from Table 6, the dose results using the moving source method are in all cases slightly smaller than those obtained from the moving sample configuration. This difference can be explained if one examines the two methods more closely. In the moving sample method, all paths are taken to be perpendicular to the sample surface and are, therefore, all of minimum length and result in maximum dose. In the moving source case, oblique paths are also measured and although these are not markedly different from normal paths for the source-detector distances used, there is some difference. Therefore the total dose calculated is smaller. One would expect, in fact, that as the source-detector distance increased, the two results would come closer together. However, even for the

Table 6 — Comparison of Doses Obtained in Moving Source Geometry With Those from Moving Sample Geometry

(Mesh Width: 0.3 in. × 0.3 in.)

Equipment	Moving Source Dose, Mev				Source Detector Distance, in.	Moving Sample Dose, Mev			
	May Flare	Sept. Flare	Feb. Flare	Van Allen		May Flare	Sept. Flare	Feb. Flare	Van Allen
NASA SA 105	4.18×10^{11}	9.61×10^{8}	9.08×10^{10}	4.27×10^{4}	48	4.69×10^{11}	1.03×10^{9}	9.66×10^{10}	4.56×10^{4}
NAA – section with stainless steel sides	1.14×10^{12}	1.32×10^{9}	1.25×10^{11}	5.62×10^{4}	18	1.36×10^{12}	1.48×10^{9}	1.41×10^{11}	6.25×10^{4}
NAA – section with Al sides	1.50×10^{12}	1.43×10^{9}	1.42×10^{11}	6.01×10^{4}	18	1.42×10^{12}	1.49×10^{9}	1.44×10^{11}	6.30×10^{4}

case where source and detector are only 18 in. apart the deviation does not exceed 20%.

It would appear, therefore, that it is feasible to use the gamma-ray probe technique in an uncollimated geometry and to obtain from it doses which differ at most by 30% from doses obtained when collimation is used. In most of the cases studied, the deviation is much less than this.

6. PROTON DOSE AND THE ATOMIC NUMBER OF THE ATTENUATING MATERIAL

6.1 GENERAL CONSIDERATIONS

As pointed out previously (Sections 2 and 3), proton attenuation is better characterized by the number of electrons in the path of the protons than by the total mass of material. However, as Fig. 2 shows, even when electron density is used there is still some variation of proton attenuation with the atomic number of the material.

Eq. 1 is an expression for the stopping power, S_i, of a material, i. Bethe[7] has derived a formula for S_i which, for protons, is given by

$$S_i = \frac{4\pi e^4 N_0 (Z/A)_i}{M_e v_p^2} \left[\ln \left(\frac{2M_e v_p^2}{I_i} \right) - \ln (1-\beta^2) - \beta^2 \right] \qquad (9)$$

where e = electronic charge

N_0 = Avogadro's number

$(Z/A)_i$ = nuclear charge to mass ratio of material i

M_e = rest mass of the electron

v_p = proton velocity

$\beta = v_p/C$

I_i = mean ionization potential of material i.

The units of S_i are Mev/g/cm^2.

Table 7 — Proton Dose* Results Using Several Range-Energy Tables – NASA Voltage Supply Box Scanned in Collimated Geometry

Flare	Cu	Al	CH_2
May 10, 1959	2.21×10^{11}	1.79×10^{11}	1.37×10^{11}
Sept. 3, 1960	8.77×10^{8}	8.24×10^{8}	7.67×10^{8}
Feb. 23, 1956	8.24×10^{10}	7.88×10^{10}	7.46×10^{10}
Van Allen belt	3.97×10^{4}	3.76×10^{4}	3.53×10^{4}

*Doses are in Mev.

age Z much closer to aluminum than either copper or CH_2, the dose errors to be expected because of the use of the proton range-energy table for aluminum would be less than those cited, even for proton spectra like those of the May 10, 1959 solar flare.

As a more extreme illustration of the relative independence of the proton dose (of the material whose proton range table is used in the calculations), the doses through various thicknesses of aluminum have been computed using three test range-energy tables. Table 8 gives the proton dose results for aluminum thicknesses from 1/4 in. to 3 in. for the usual four proton spectra. Even in the worst case (3 in. of aluminum for the flare of May 10, 1959), the error does not exceed 40% even though the attenuating material is actually all aluminum.

The results obtained in this study lead us to the conclusion that one can use an "average" proton attenuating material in calculating proton dose for the heterogeneous equipment pieces to be found in space vehicles. If, in scanning a complete vehicle, certain areas are known to be composed of given materials only, the range-energy table or expression used in the calculational procedure can be changed to fit the given circumstances. However, as the results shown in Table 8 seem to indicate, this may be necessary only if these known materials have very high or very low (e.g., hydrogen) values of Z.

Table 8 — Proton Dose* Results, Using Several Range-Energy Tables – As Calculated for Several Thicknesses of Aluminum

	Range Table Used	Aluminum Thicknesses 0.25 in.	0.5 in.	2 in.	3 in.
May 10, 1959	Cu	7.72×10^{11}	3.61×10^{11}	2.87×10^{11}	1.17×10^{11}
Sept. 3, 1960	Cu	1.25×10^{9}	1.03×10^{9}	5.25×10^{8}	3.76×10^{8}
Feb. 23, 1956	Cu	1.14×10^{11}	9.35×10^{10}	5.83×10^{10}	4.56×10^{10}
Van Allen belt	Cu	5.41×10^{4}	4.57×10^{4}	2.54×10^{4}	1.96×10^{4}
May 10, 1959	Al	6.88×10^{11}	2.93×10^{11}	2.07×10^{11}	8.45×10^{10}
Sept. 3, 1960	Al	1.22×10^{9}	9.77×10^{8}	4.64×10^{8}	3.23×10^{8}
Feb. 23, 1956	Al	1.10×10^{11}	8.98×10^{10}	5.36×10^{10}	3.94×10^{10}
Van Allen belt	Al	5.30×10^{4}	4.39×10^{4}	2.28×10^{4}	1.76×10^{4}
May 10, 1959	CH_2	5.83×10^{11}	2.20×10^{11}	1.51×10^{11}	6.09×10^{10}
Sept. 3, 1960	CH_2	1.16×10^{9}	9.19×10^{8}	4.13×10^{8}	2.74×10^{8}
Feb. 23, 1956	CH_2	1.05×10^{11}	8.51×10^{10}	4.91×10^{10}	3.36×10^{10}
Van Allen belt	CH_2	5.08×10^{4}	4.15×10^{4}	2.08×10^{4}	1.59×10^{4}

*Doses are in Mev.

7. THE EFFECT ON DOSE CALCULATIONS OF THE VARIATION OF SEVERAL SYSTEM PARAMETERS

7.1 GAMMA-RAY SOURCE

Among the possible isotopes which might be used as gamma-ray sources in the probe technique, only Co^{60} and Cs^{137} appear suitable from the point of view of availability, adequate lifetime, and simple spectrum. In general, Co^{60} is the preferred isotope because it is available in wire form and has a slightly higher percentage of its total cross section as Compton scattering than does Cs^{137}. These reasons become more important as the atomic number of the attenuating material increases. Cs^{137} usually comes in the form of a solution, or at best, as a powder. Therefore, it is more difficult to make up into a suitable source.

The lower energy of the gamma ray from Cs^{137} does, however, hold forth the possibility of being able to differentiate smaller differences of electron density. Therefore, a Cs^{137} powder source from a solution of $Cs^{137}Cl$ was prepared and used to determine the values of effective Compton cross section given in Section 3.2 and in Table 9.

The results given in Table 9 show that the difference between the effective Compton cross section and the theoretical value for Cs^{137} is much larger than it is for Co^{60}. This follows from the fact (see Section 3) that Cs^{137} gammas can be scattered through a larger angle than Co^{60} gammas and still be admitted by the energy discriminating system. Therefore, for uncollimated geometry, Cs^{137} offered no

Table 9 — Theoretical and Effective Compton Cross Sections for Co^{60} and Cs^{137}

	Compton Cross Sections $\times 10^{-24}$ cm^2/electron	
	Theoretical	Effective
Co^{60}	0.186	0.154
Cs^{137}	0.254	0.174

advantage over Co^{60}, and since Co^{60} does have the other advantages mentioned above, it was used exclusively in examining actual equipment.

7.2 SCINTILLATOR CRYSTAL SIZE

The scintillation crystals used as gamma-ray detectors in this study were prepackaged, NaI(Tl) cylindrical crystals manufactured by the Harshaw Chemical Co. Experiments were carried out using crystals of various sizes ranging from 1/2 in. by 1/2 in. to 3 in. by 2 in.

The dose results for a series of such measurements for an array of 1 in. aluminum blocks spaced 1 in. apart are given in Table 10. These show that for this array the crystal sizes used appear to have little influence on the calculated dose. Similar results shown in Table 11 were obtained for an array of aluminum blocks spaced distances of 1/8, 1/4, 1/2, and 1 in. apart. The data in this case were taken for the 1 in. by 1 in. and 2 in. by 2 in. crystals.

Although Table 10 shows that the 1/2 in. by 1/2 in. crystals give good dose results, the gamma-ray spectrum obtained for Co^{60} gammas using this crystal was not an acceptable one. This resulted from the small size of the crystal and its consequent inability to stop completely a sufficient number of Co^{60} gammas. The poor spectrum prevented the Spectrostat from remaining "locked on" to the gamma peak, and as a result serious drifting occurred. The 1/2 in. by 1/2 in. crystal was not used in subsequent scans. The other crystals did give acceptable spectra

Table 10 — Doses* Behind an Array of 1-in. Al Blocks Spaced 1 in. Apart – Variation With Crystal Size

Flare	Ideal (i.e., Calculated Case)	1/2 × 1/2 in. Crystal	1 × 1 in. Crystal	3 × 2 in. Crystal
May 10, 1959	1.44×10^{12}	1.42×10^{12}	1.44×10^{12}	1.44×10^{12}
Sept. 3, 1960	1.41×10^{9}	1.34×10^{9}	1.34×10^{9}	1.35×10^{9}
Feb. 23, 1956	1.40×10^{11}	1.40×10^{11}	1.40×10^{11}	1.40×10^{11}
Van Allen belt	5.72×10^{4}	5.67×10^{4}	5.67×10^{4}	5.72×10^{4}

*Doses are in Mev.

Table 11 — Doses* Behind an Array of 1-in. Al Blocks Separated by 1/8, 1/4, 1/2, and 1 in. Spaces – Variation With Crystal Size

Flare	Ideal (i.e., Calculated Case)	1 × 1 in. Crystal	2 × 2 in. Crystal
May 10, 1959	9.08×10^{11}	8.93×10^{11}	8.87×10^{11}
Sept. 3, 1960	1.10×10^{9}	1.10×10^{9}	1.10×10^{9}
Feb. 23, 1956	1.13×10^{11}	1.12×10^{11}	1.12×10^{11}
Van Allen belt	4.77×10^{4}	4.78×10^{4}	4.80×10^{4}

*Doses are in Mev.

and the choice of the 2 in. by 2 in. crystal for the automatic scans of equipment pieces was made mainly on the basis of counting rate. This crystal gave a counting rate four times higher than the 1 in. by 1 in. crystal. Although there possibly may be some advantage in better delineation of structure (see Section 8) in using the smaller crystal (1 in. by 1 in.), counting rate considerations dictated the use of the 2 in. by 2 in. crystal.

7.3 MESH SIZE

The gamma-probe method, when used on heterogeneous structures, can be time consuming and tedious unless it can be shown that scanning over a fairly large mesh gives acceptable dose results. Scanning over a very small mesh will, of course, delineate the character of the sample more exactly and, in general, will result in the calculation of a larger dose. However, if the dose is found to be not too sensitive to mesh size, acceptable dose values may still be obtained, even though a fairly coarse mesh width is used. Several equipment pieces and spacecraft sections have been scanned at a variety of mesh widths from 0.2 in. by 0.2 in. to 1 in. by 0.5 in. The first number describing the mesh size is the distance traversed by the source/sample table in the time in which a gamma-ray measurement is made (usually 1 sec). The second number listed is the distance the table moves in the transverse direction between traverses. Hence, a 0.5 by 0.5 mesh means that the table moves 0.5 in. in the horizontal direction over which distance the total number of gamma rays reaching the detector is counted and recorded. Such measurements are made over the entire horizontal traverse and then the table advances vertically 0.5 in. and another horizontal traverse is made. The run is continued in this manner until the entire piece is scanned.

The dose results from a number of scans in which the mesh size was varied are given in Tables 12 and 13. The results show that even for a very heterogeneous sample, like the NASA SA 105 piece, the difference in dose calculated over the range of mesh sizes used is at most 20% for the very sensitive May 10, 1959 flare.

Table 12 — Doses* Behind NASA SA 105 Equipment – Variation With Mesh Size

Flare	Mesh Size, in. 0.2 × 0.2	0.3 × 0.3	0.5 × 0.5	1.0 × 0.5
May 10, 1959	5.25×10^{11}	4.69×10^{11}	4.74×10^{11}	4.20×10^{11}
Sept. 3, 1960	1.07×10^{9}	1.03×10^{9}	1.03×10^{9}	1.02×10^{9}
Feb. 23, 1956	9.92×10^{10}	9.66×10^{10}	9.66×10^{10}	9.45×10^{10}
Van Allen belt	4.70×10^{4}	4.56×10^{4}	4.55×10^{4}	4.50×10^{4}

*Doses are in Mev.

Table 13 — Dose* Behind North American Aviation Space Vehicle Sections – Variation With Mesh Size

Mesh Size, in.	Flare May 10, 1959	Sept. 3, 1960	Feb. 23, 1956	Van Allen Belt
	3/4-in. Thick Honeycomb – Al Sides			
0.2 × 0.2	1.39×10^{12}	1.49×10^{9}	1.42×10^{11}	6.25×10^{4}
0.3 × 0.3	1.42×10^{12}	1.49×10^{9}	1.44×10^{11}	6.30×10^{4}
0.5 × 0.5	1.31×10^{12}	1.45×10^{9}	1.39×10^{11}	6.14×10^{4}
	2-in. Thick Honeycomb – Stainless Steel Sides			
0.2 × 0.2	1.21×10^{12}	1.43×10^{9}	1.34×10^{11}	6.04×10^{4}
0.3 × 0.3	1.36×10^{12}	1.48×10^{9}	1.41×10^{11}	6.25×10^{4}
0.5 × 0.5	1.26×10^{12}	1.44×10^{9}	1.37×10^{11}	6.10×10^{4}

*Doses are in Mev.

For more homogeneous samples like the North American Aviation vehicle sections, the deviation is 10% or less even for that flare.

Therefore, it is concluded that it is possible to obtain reasonable proton dose values using a fairly coarse mesh even for decidedly heterogeneous specimens.

7.4 SOURCE-SAMPLE-DETECTOR DISTANCES

Gamma-ray scans were carried out for a number of different source-sample-detector configurations.

The three principal configurations tested were:

1. Source close to the sample (usually 1 in. away)
2. Sample midway between the source and the detector
3. Sample close to the detector (usually 1 in. away).

The source-detector distance in most of the scans was 20 in.

A graphical representation of a series of such scans is given in Fig. 3 for the array of 1-in. aluminum cubes spaced 1/8, 1/4, 1/2, and 1 in. apart. As can be seen, the configuration in which the source is close to the sample gives the best delineation of array structure. With the sample midway between source and detector more averaging occurs. The poorest resolution of structure occurs when the sample is close to the detector. Good structure delineation is achieved, as shown in Fig. 4, when the sample (a composite one this time) is placed close to both source and detector. As can be seen, this is better resolution than was obtained for the sample midway between source and detector in Fig. 3, though not quite so good as when the source is close to the sample in the latter figure. Similar results on structure resolution have been obtained for a variety of arrays in which the thickness and kind of material have been varied as well as the spacing between the components of the array.

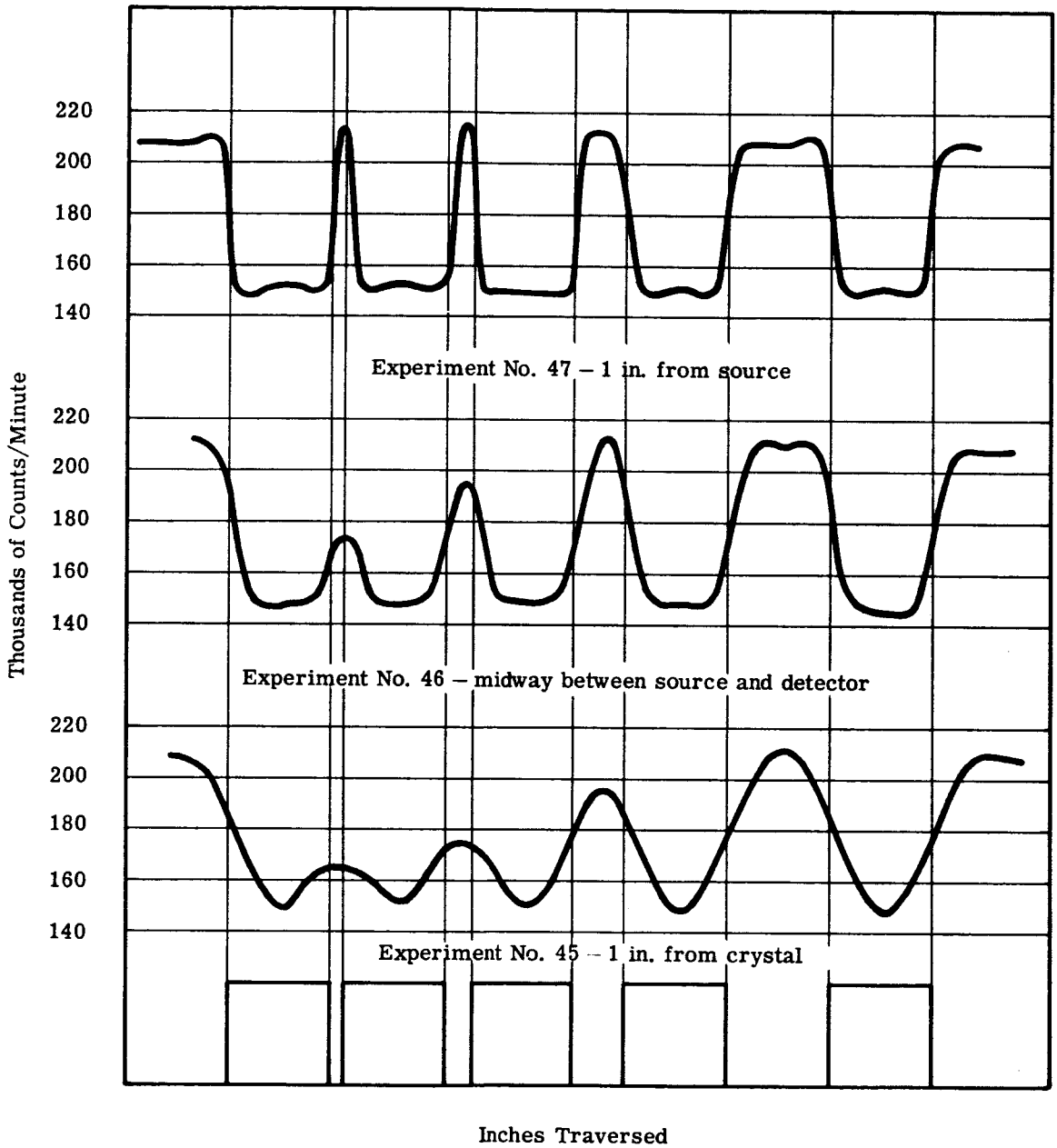

Fig. 3 — Results of a gamma-ray scan of a 1-in. Al cube array spaced 1/8, 1/4, 1/2, and 1 in. A 1 in. × 1 in. crystal and a 5-mc Co^{60} source were used.

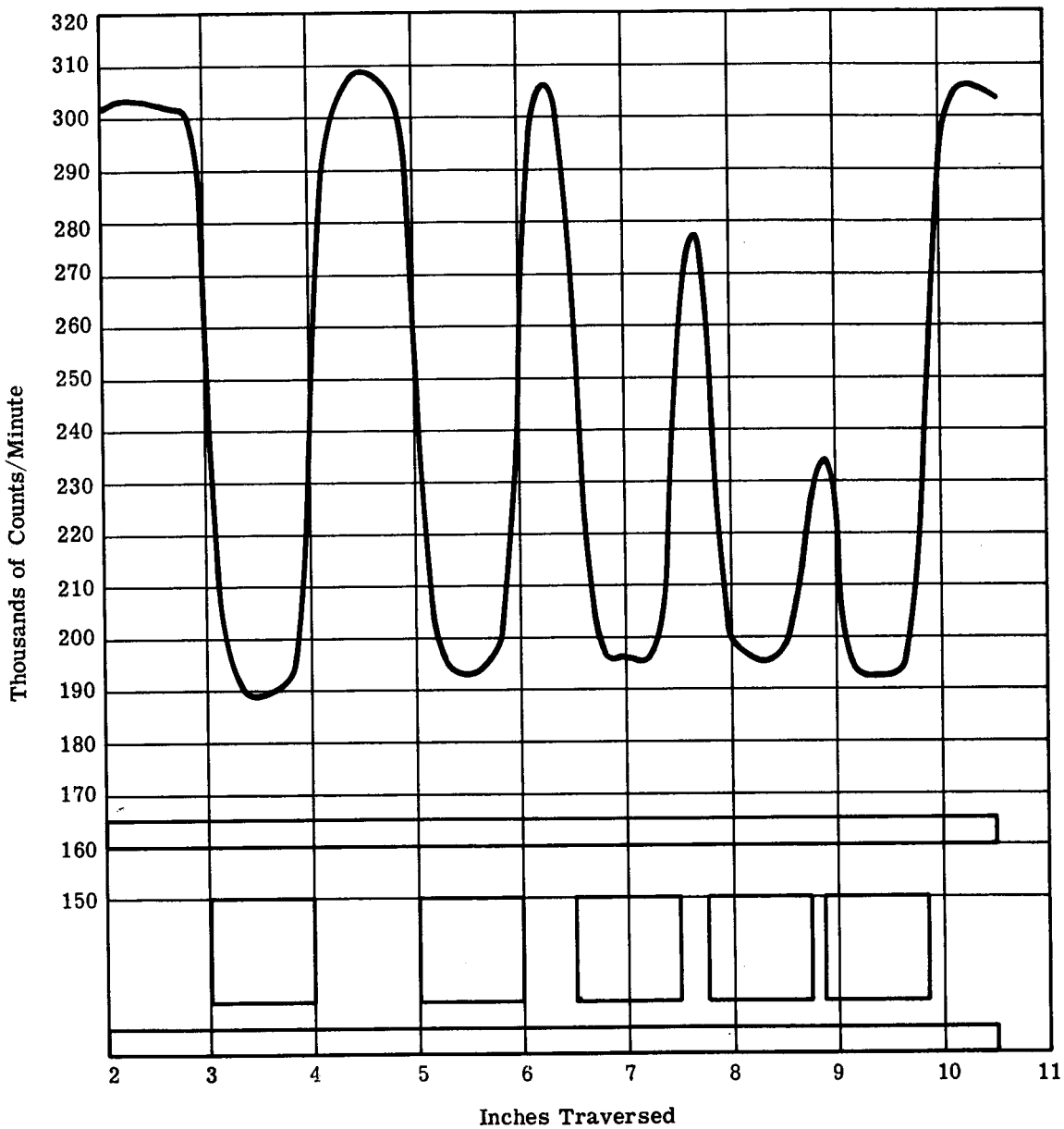

Fig. 4 — Results of a gamma-ray scan of a 1-in. Al cube array spaced 1/8, 1/4, 1/2, and 1 in. with the addition of 1/4 in. of Al in front of the source and in front of the detector. A 1 in. × 1 in. crystal and a 15-mc Cs^{137} source were used.

The doses calculated from the scan data obtained in the three different configurations show that the highest dose is obtained for the configuration in which the source is near the sample. This is to be expected since, for this case, the probe technique does the least amount of averaging. The dose results for all three configurations, as given in Table 14 for the aluminum array with varying spacing, also show that the dose is less sensitive to the relative position of source, sample, and detector than Fig. 3 would indicate. However, when the source is close to the sample, the dose obtained is closest to the ideal (i.e., calculated) case for all the arrays tested.

This result plus the obvious superiority of the "source close to sample" configuration in delineating structure make it the best choice for probing spaceship sections and equipment. To be able to pick out small openings or thin spots in a space vehicle and its equipment, the preferred method is to place the source close to the sample surface. The placement of the detector is not very critical and it may be placed as close as about 6 in. behind the sample. In the scans made of space vehicle sections and equipment, the source in all cases has been placed close to the sample.

Table 14 — Dose* Behind an Array of 1-in. Al Blocks Separated by 1/8, 1/4, 1/2, and 1 in. Spaces (1 in. × 1 in. Crystal) — Variation With Source-Sample-Detector Distance

Flare	Ideal (i.e., Calculated Case)	Sample 1 in. from Source	Sample in Center	Sample 1 in. from Detector
May 10, 1959	9.08×10^{11}	8.93×10^{11}	6.77×10^{11}	7.04×10^{11}
Sept. 3, 1960	1.10×10^{9}	1.10×10^{9}	1.02×10^{9}	1.08×10^{9}
Feb. 23, 1956	1.13×10^{11}	1.12×10^{11}	1.02×10^{11}	1.06×10^{11}
Van Allen belt	4.77×10^{4}	4.78×10^{4}	4.48×10^{4}	4.73×10^{4}

*Dose is in Mev.

8. GAMMA-PROBE TECHNIQUE AND HOMOGENIZATION

In previous calculations made at United Nuclear of the attenuation of protons in space capsule equipment, it was assumed that the equipment was homogeneously distributed within the vehicle. However, recognizing that neither the equipment nor its distribution was actually homogeneous, its areal density was reduced by 30% to account for the increased transmission through low density areas.

In order to see how valid such a reduction is, the dose results from gamma probe scans were compared to doses calculated assuming the sample to be homogeneous and having an areal density given by its dimensions and mass. The results of the comparison are given in Table 15 for two sample flares for the two NASA pieces scanned as well as for the North American Aviation capsule sections. The "homogenized" dose values were obtained from PROBE code calculations for various thicknesses of aluminum.

The comparison shows that it would not be unrealistic to use the homogenized dose value for the two NAA spacecraft sections. An examination of their structure does show them to be quite homogeneous. For the NASA Voltage Supply Box, whose internal structure is still fairly homogeneous (it is "potted" in epoxy resin), the assumption of a 30% reduction in areal density would probably be valid. However, for the more heterogeneous NASA SA 105 piece, assuming full density would result in a dose error of nearly a factor of three for the May 10, 1959 flare. In order to correct for this, one would have to assume that the areal density of this piece of equipment was nearly half the homogeneous value.

Table 15 — Comparison of Calculated Dose* Based on Homogenized Density with Calculated Dose Based on Gamma-Probe Scans

	Calculated Density, g/cm^2	Electron Density (if all Al) e/cm^2	May 10, 1959 Flare		Feb. 23, 1956 Flare	
			Homogenized	Scan	Homogenized	Scan
NASA Voltage Supply	6.30	1.83×10^{24}	1.08×10^{11}	1.79×10^{11}	7.40×10^{10}	7.88×10^{10}
NASA SA 105	5.50	1.60×10^{24}	1.44×10^{11}	3.95×10^{11}	7.77×10^{10}	9.29×10^{10}
NAA – 3/4-in. Honeycomb (Al sides)	0.47	0.14×10^{24}	1.42×10^{12}	1.39×10^{12}	1.47×10^{11}	1.42×10^{11}
NAA – 2-in. Honeycomb (SS sides)	0.84	0.23×10^{24} (if SS)	1.18×10^{12}	1.21×10^{12}	1.37×10^{11}	1.34×10^{11}

*Doses are in Mev.

This brief comparison serves to point up the utility of the gamma-probe technique. The method can give the proper proton dose to be expected behind the samples measured even though they may differ widely in homogeneity. In addition, no guess need be made as to the proper reduction in density required to compensate for the heterogeneous construction and distribution of space vehicle equipment.

9. CONCLUSIONS

The results of the study described in this report demonstrate the feasibility and practicality of using the gamma-probe technique for the determination of the shielding effectiveness of space vehicles and their equipment.

It has been shown that the method gives dose values, in calculable cases, consistent with analytical results.

The feasibility of scanning in uncollimated geometry has been demonstrated with both moving samples and moving sources. By use of an effective Compton cross section, dose values comparable to those in collimated geometry can be obtained. The ability to scan in uncollimated geometry reduces tremendously the amount of time needed to measure a complete capsule, besides simplifying considerably the apparatus required.

It has been shown that mesh sizes as large as 1 in. can give dose results comparable to those obtained by using much smaller mesh widths, even for heterogeneous samples. It may be possible to use even larger meshes in actual vehicle scans and thus reduce running time further.

It was found that for realistic capsule configuration, an "average" material, such as aluminum, can be used in calculating the proton dose from the measured electron densities.

The spatial details of heterogeneous structures can be delineated by the gamma-probe method even in uncollimated geometry. Therefore, the method can be used to detect unsuspected shielding "thin spots" in the spacecraft walls and equipment. The best detail is obtained when the source is close to the sample. Dose results, however, are not as sensitive to source-sample-detector distances.

On the basis of the results of this study, recommendations have been made for a system to scan a complete space capsule. In addition, it has been suggested to NASA that the gamma-probe measurements of individual space vehicle components be continued and expanded. The results of such measurements then can be used to obtain average electron density distributions for single pieces of equipment. An analysis of the individual density distributions then may lead to the definition of classes of equipment, all members of a class being described, for shielding purposes, by a single density distribution.

10. APPENDIX – DESCRIPTION OF THE AUTOMATIC SCANNING SYSTEM

The automatic scanning system was designed to measure the transmission of gamma rays through various specimens with either a moving source or a moving sample. The table motion and gamma-ray counting were to be continuous. The counts for succeeding seconds are accumulated alternately in each of two recording scalers. The scaler that is idle during any second is read onto punched tape and is reset during this second in which it is not recording. A photograph of the entire system is shown in Fig. 5.

10.1 THE SCANNING TABLE

The scanning table was designed to support either specimens to be scanned or a gamma source and its lead shielding. It is driven smoothly horizontally, stops at the end of a traverse, rises a preset distance, stops again and finally returns on a horizontal traverse. Its scanning capabilities are 2 ft by 2 ft and it can support a load of 100 lb in any position at any extension.

The guide rails are made of 1/4-in. by 3-in. mild steel with 2-in. diameter ball bearings for wheels. As indicated in Fig. 6, a carriage supported between four rails carries wheels which in turn support two other rails fixed to the table.

The two drives (horizontal and vertical) are actuated by Slo-syn motors (trademark of the Superior Electric Co., meaning slow and synchronous). These motors rotate at 72 rpm on 60 cycle current and start and stop in about 1 cycle. The

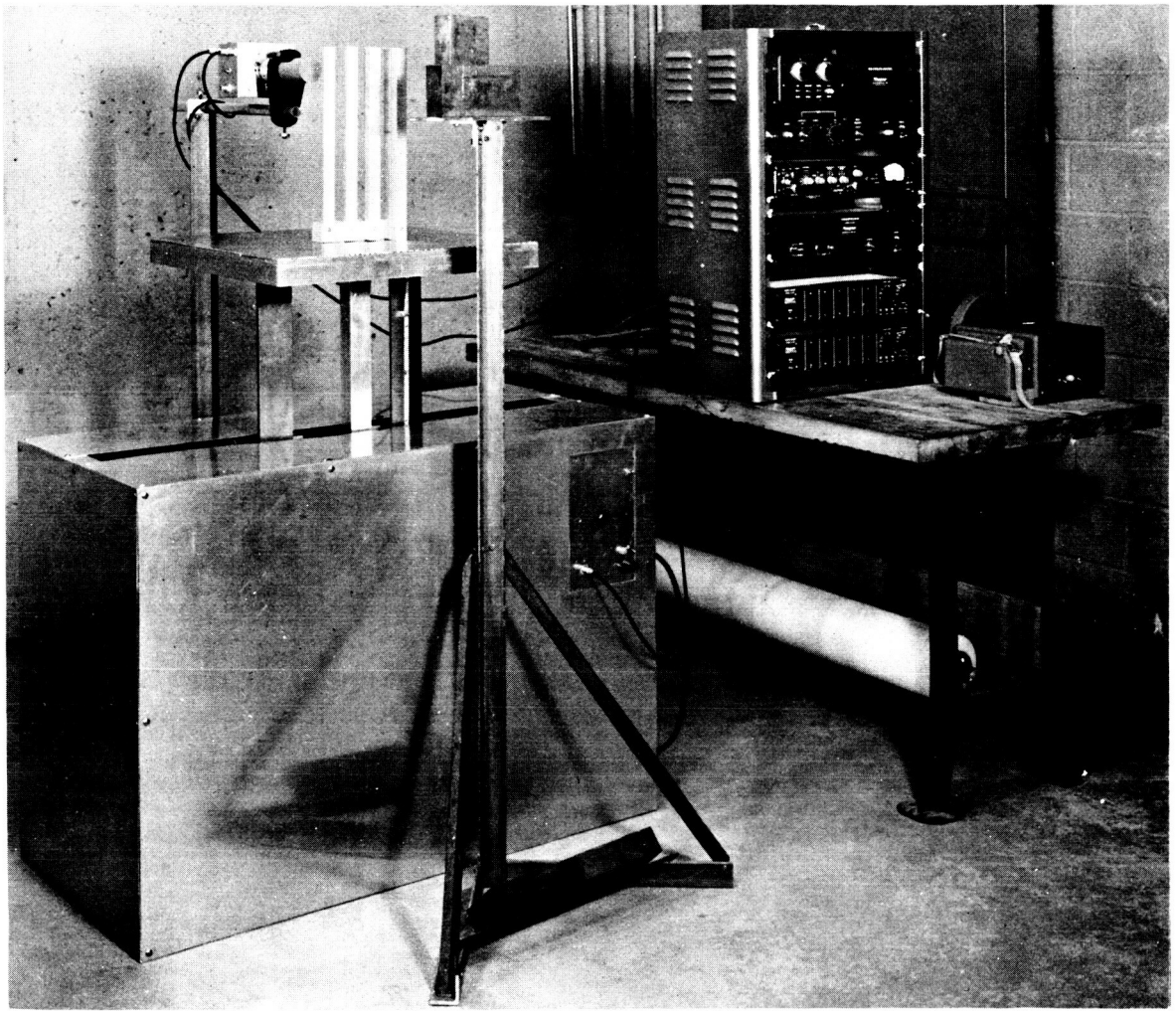

Neg. No. 4442

Fig. 5 — The gamma-probe scanning system

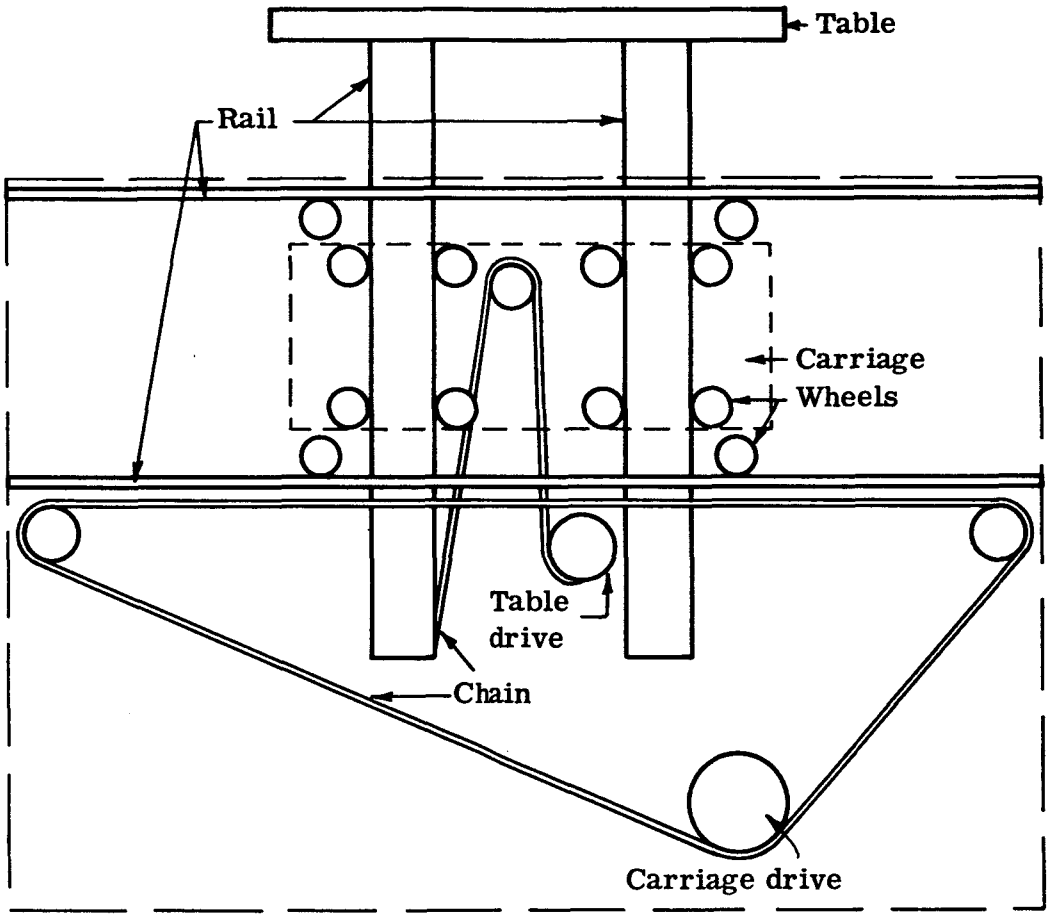

Fig. 6 — Schematic of the scanning table drive mechanisms

horizontal drive motor runs a series of sprockets, any one of which can be meshed with a roller chain to drive the carriage at speeds of 0.1, 0.2, 0.3, 0.4, 0.5, 0.6, and 0.75 in./sec. The vertical drive motor actuates a switch with each 0.1-in. rise of the table, and this switch, in turn, actuates a stepping switch which controls the total rise of the table. This incremental vertical displacement can be preset any where from 0.1 in. to 1.0 in. in increments of 0.1 in.

A set of relays and switches are connected so that a relay is operated at the end of a horizontal traverse to transfer power from the horizontal drive motor to the vertical one. A relay flip-flop reverses the horizontal drive motor connections at the end of a traverse so that when this motor is next switched on it will reverse the carriage direction. The vertical drive motor operates until the stepping switch counts the preset rise, at which time power is transferred back to the horizontal drive motor. The stepping switch then resets itself in preparation for the next vertical displacement. There are limit switches on the vertical travel, the lower one to protect the machine, and the upper one to terminate the scan at a preset value of total rise.

The horizontal drive motor, through a cam and switch, also supplies clock pulses, spaced 1 sec apart, to time each gamma-counting measurement. The pulses accomplish this by turning off one scaler and turning on its partner once each second. A set of contacts on the clock switch must be actuated by either limit switch to terminate a traverse, so that the length of any traverse is an integral number of seconds. Another feature of the timing system is that the detector output is shorted whenever the table is rising so that all counting periods are one second duration even though at the end of the traverses the elapsed time between one counting position and the next may be longer.

10.2 THE COUNTING AND RECORDING SYSTEM

The majority of the electronic equipment is standard and most of it was supplied by the Hammer Electronics Co. Fig. 7 is a block diagram of the system.

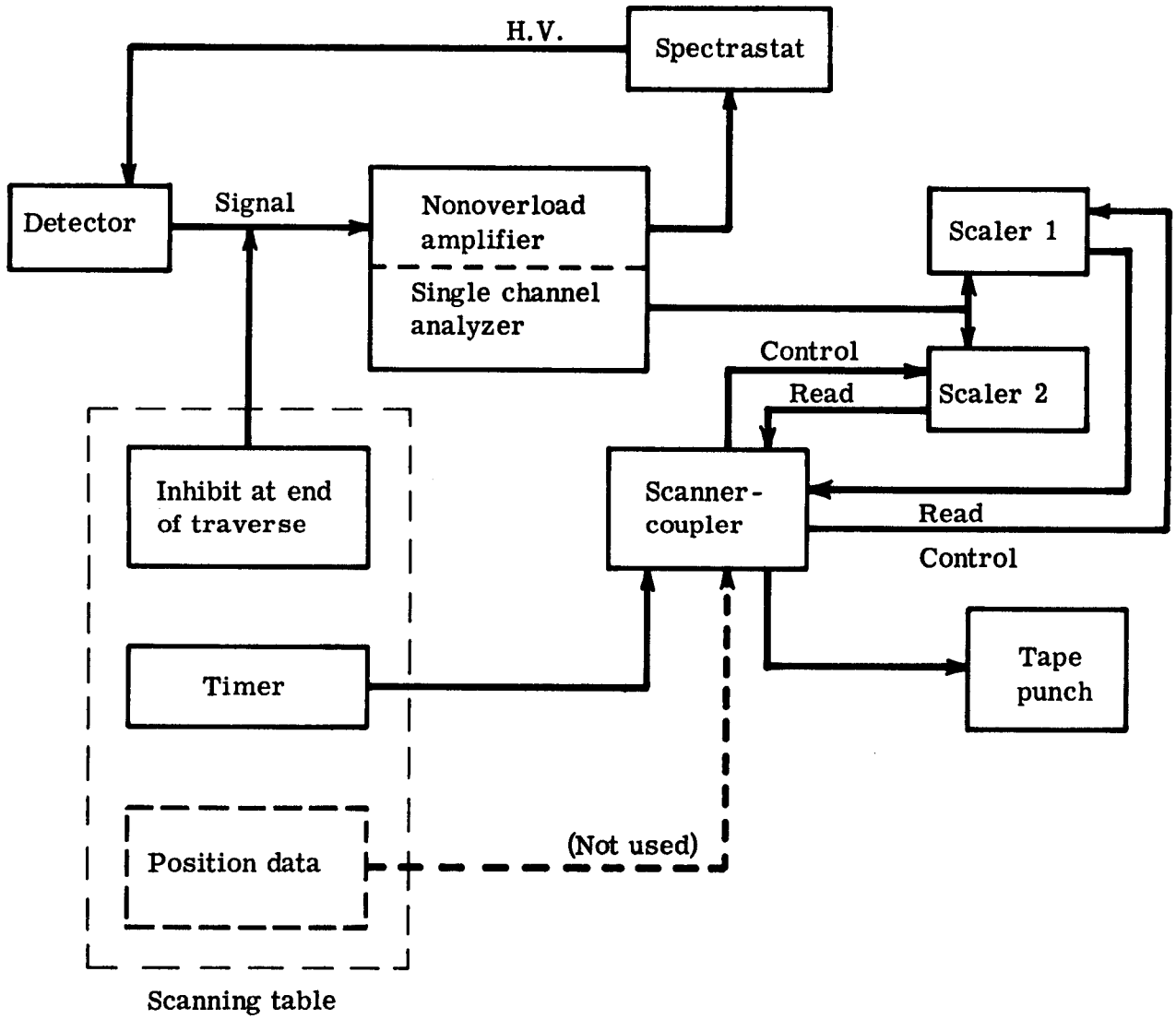

Fig. 7 — Block diagram of the electronics system

The gamma-ray detector is a scintillation counter which receives power from a Spectrastat (trademark of Cosmic Radiation Laboratories, Inc.). The "inhibit switch" grounds the detector output while the table is rising. The amplifier and pulse height analyzer send amplified pulses to the Spectrastat, but send "spikes" to the scalers only for pulses that are larger than a preset value.

The Spectrastat measures and compares the counting rates at two points on the sides of a pulse amplitude peak and adjusts the high voltage to keep those counting rates equal. The Spectrastat thus holds a peak at any predetermined value by compensating for any gain changes in the system. The system acts as a gain-stabilized scintillation counter with integral discrimination.

The scanner/coupler was made specifically for this investigation. It alternately starts one scaler and stops the other in response to the clock pulses. It also converts the d-c levels, which are the analog outputs of the scalers, to power pulses which operate the tape punch. After printing out the contents of one scaler, the coupler resets that scaler to zero. It has the capacity to print four decimal digits in addition to the scaler output each second. This capacity was specified in the event that the coordinates of each data point were to be printed out along with the gamma counts. However, it was not necessary to use this capacity in this study.

11. REFERENCES

1. H. J. Schaefer, Dosimetry of Proton Radiation in Space, U.S. Naval School of Aviation Medicine Project, MR 005.13-1002 Subtask 1, Report No. 19 (1961).
2. D. H. Robey, Radiation Shield Requirements for Two Large Solar Flares, Astronautica Acta, 6:206 (1960).
3. W. A. Gibson, Energy Removed from Primary Proton and Neutron Beams by Tissue, ORNL-3260 (Sept. 1962).
4. G. W. Grodstein, X-Ray Attenuation Coefficients from 10 kev to 100 Mev, NBS Circular 583 (Apr. 1957).
5. S. C. Freden and R. S. White, Particle Fluxes in the Inner Radiation Belt, J. Geophys. Res. 65:1377 (1960).
6. A. D. Krumbein et al., Synthesis of Minimum Weight Proton Shields, p. 48, UNC-5049 (Feb. 1963).
7. D. Halliday, "Introductory Nuclear Physics," 2nd Ed., p. 155, John Wiley and Sons, Inc., New York, 1958.
8. M. Rich and R. Madey, Range-Energy Tables, UCRL-2301 (Mar. 1954).

DISTRIBUTION

	No. of Copies
National Aeronautics and Space Administration George C. Marshall Space Flight Center Purchasing Office Huntsville, Alabama 35812 Attn: PR-RDC	40*

*Plus one reproducible.